Actinic mask imaging: Recent results and future directions from the SHARP EUV Microscope

Kenneth A. Goldberg,*[a] Markus P. Benk,[a] Antoine Wojdyla, Iacopo Mochi,[a]
Senajith B. Rekawa,[a] Arnaud P. Allezy,[a] Michael R. Dickinson,[a] Carl W. Cork,[a]
Weilun Chao,[a] Daniel J. Zehm,[a] James B. Macdougall,[a] Patrick P. Naulleau,[a] and Anne Rudack[b]
[a]Lawrence Berkeley National Laboratory, 1 Cyclotron Rd., Berkeley, CA USA 94720;
[b]SEMATECH, 257 Fuller Rd. Suite 2200, Albany, NY USA 12203

ABSTRACT

The SEMATECH High Numerical Aperture Actinic Reticle Review Project (SHARP) is a synchrotron-based extreme ultraviolet (EUV) microscope dedicated to photomask research. SHARP has been operational and serving users since June, 2013, and in eight months, SHARP has recorded over 71,000 high-resolution images. Exposure times are 5 to 8 seconds, and 8 or more through-focus series can be collected per hour at positions spanning the entire mask surface. SHARP's lossless coherence-control illuminator and variable numerical aperture (NA) enable researchers to emulate the imaging properties of both current and future EUV lithography tools. SHARP's performance continues to improve over time due to tool learning and upgraded capabilities, described here. Within a centered, 3-μm square image region, we demonstrate an illumination power stability above 99%, and an average uniformity of 98.4%. Demonstrations of through-focus imaging with various illumination coherence settings highlight the capabilities of SHARP.

Keywords: extreme ultraviolet, EUV, mask, microscope, coherence, zoneplate, imaging

1. INTRODUCTION

The SEMATECH High-NA Actinic Reticle review Project (SHARP) microscope is the successor to the SEMATECH Berkeley Actinic Inspection Tool (AIT) and occupies the same synchrotron, bending magnet beamline at Lawrence Berkeley National Laboratory's (LBNL) Advanced Light Source (ALS). SHARP was created by an industry/government partnership to provide advanced research and development capabilities. It utilizes an all-EUV "actinic" illumination and imaging system. Like AIT, the SHARP microscope uses off-axis Fresnel zoneplate lenses to project EUV images with high magnification (typically 900×) and diffraction-limited quality. Yet SHARP is a ground-up re-design of the AIT concept and achieves 150 times higher power with the same source due to an efficient illuminator design and a reduction in the number of mirrors by two.

SHARP is used to study nearly every aspect of EUV mask technology, including programmed and native defect detection and sensitivity, mask cleaning and repair strategies, through-focus defect printability, horizontal-vertical (HV) bias arising from off-axis illumination, optical proximity correction and pattern enhancement, multilayer and absorber architecture, multilayer surface roughness and pattern line-edge roughness, phase-shifting mask architectures, and more.[1–5]

1.1 The role of SHARP

A host of inspection technologies have contributed to progress in EUV mask research,[6] including tools to improve defect detection and verify mitigation. Clearly the need for mask metrology tools offering high scanning speed, and other benefits will persist. Yet EUV photomasks are highly tuned to the wavelength and illumination profiles used in lithography. Non-actinic (that is, non-EUV-wavelength) inspection technologies, such as scanning electron-microscopy (SEM), photo-electron microscopy (PEEM), atomic-force microscopy (AFM), and deep-ultraviolet inspection techniques miss subtle optical effects that can only be accurately characterized at the operational wavelength. This may be especially true for the approaching, ever smaller pattern design rules (at and below 16-nm) and for so-called phase-defects resulting from small bumps and pits in the multilayer coating or subtrate.

SHARP is a unique research prototype, designed to provide a window on EUV lithography mask research at current or future technology nodes. Its high specifications and current availability enable it to participate in ongoing strategic photomask decision-making. SHARP is designed for use with a narrow-band, narrow-divergence source, and it is installed at a synchrotron light source where it can be accessed by participating industrial or academic, research teams.

2. SHARP'S OPTICAL SYSTEM

SHARP utilizes an all-EUV optical system, relying on reflective optics for the illuminator, and diffractive, high-magnification zoneplate objective lenses for the image projection. SHARP's source, illuminator, and projection optics have been described previously.[1] This section provides a brief overview, for context.

2.1 Bending-magnet source

The source for SHARP is a synchrotron bending magnet with a monochromator that provides EUV light with a tunable wavelength and an adjustable bandwidth $\lambda/\Delta\lambda$, set to 1/1450 at 13.5-nm wavelength. The measured EUV, in-band power at the beamline's intermediate focus is 14 μW under normal operating conditions.

2.2 Three-mirror illuminator with two dynamic elements

In the illuminator, there are three multilayer-coated mirrors used to (1) re-image the intermediate focus spot onto the mask with 10× demagnification, (2) dynamically fill the angular pattern, and (3) sweep out a pattern that creates uniform illumination across the mask region of interest. The illuminator is shown schematically in Fig. 1. The M_A mirror is a two-axis, angle-scanning MEMS device customized for use at EUV wavelengths and placed at the intermediate focus of the beamline. M_B is a flat folding mirror that directs the beam upward into M_C. The M_C mirror is an off-axis ellipsoid designed to concentrate all of the light leaving M_A onto a single position on the mask. M_C has a graded Mo/Si multilayer coating and a shape that allows it to illuminate the mask from 1–19° off-axis, and to span an azimuthal range appropriate for ±25° rotation of the plane of incidence at 4xNA values up to 0.625. M_C also serves as an illumination uniformity scanner: it is mounted to an *xy* tilt stage that scans a small angle pattern (tens of μrad) during each exposure.

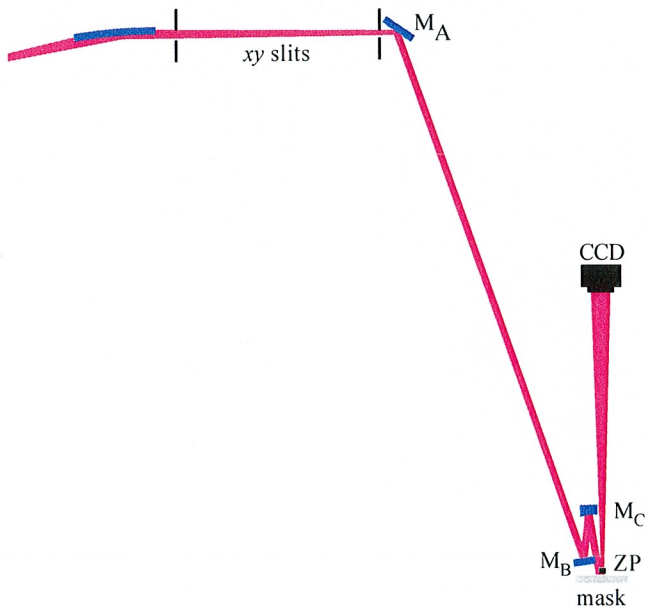

Figure 1. The beam path through the SHARP microscope's illuminator and objective, not to scale. A pair of slits condition the divergence angle and spot size of the incident beam. M_A is a scanning MEMS mirror that directs the beam downward onto a folding mirror, M_B. M_C is an off-axis ellipsoid that can illuminate the mask with a range of angles up to 19° off-axis. An array of zoneplate objective lenses is held by an independent *xyz* stage, a few hundred microns above the mask surface. The Zoneplate in use projects a high-magnification image directly onto the CCD camera.

2.3 Zoneplate objective lenses

Fresnel zoneplate lenses (typically 100-μm diameter) project the image of the illuminated mask surface onto a 1-inch EUV CCD detector with 900× or higher magnification. The individual lenses are binary holograms of a single off-axis lens, created by electron-beam lithography, and described in detail in Ref. 1. Within the array of available zoneplates, the focal lengths range from 270 to 2000 μm, with 500 μm being the nominal distance for 4xNA values at and below 0.35. The incident beam illuminates a small region of the mask, and the lenses capture the reflected light and project it directly upward to the CCD, a distance of approximately 450 mm above the mask surface.

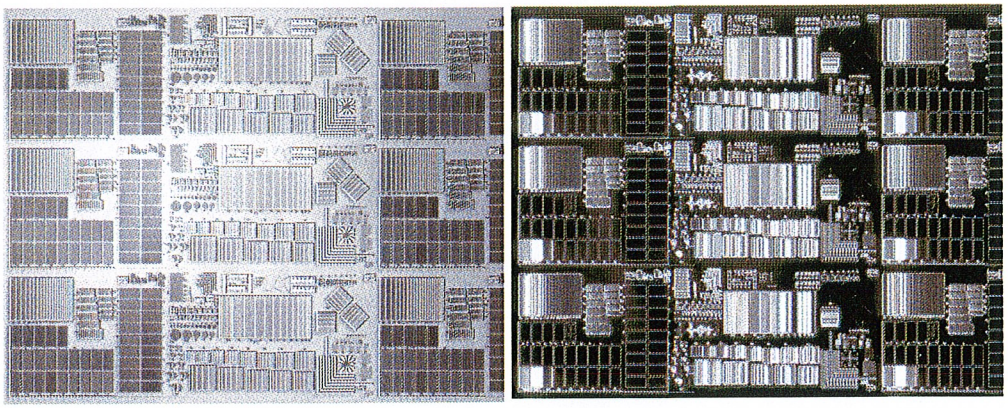

Figure 2. Visible-light microscope images of a patterned, experimental test mask. **(Left)** Brightfield, through-the-lens illumination. **(Right)** Darkfield illumination from two LED diodes positioned to illuminate the mask from the *x* and *y* directions, respectively.

3. MASK NAVIGATION TOOLS

Owing to the small field of view of EUV high-resolution imaging (30 μm is typical), finding ways to efficiently navigate the mask surface is important for experimental throughput. SHARP operators rely on patterned-absorber or buried, phase-shifting fiducial markings to define the two-dimensional coordinate system of the mask surface. While some experimental masks are designed with labeled patterns, others such as blanks, and those with high pattern density present a greater challenge.

SHARP's mask *xyz* stage utilizes magnetic position encoders, selected to avoid scattering light into the chamber. Once the mask fiducial positions have been found and a coordinate transform established, the encoders provide position accuracy below 10 μm across the full mask area. Fine positioning and focusing, relies on the tool operator to identify the measurement positions by eye.

SHARP has a built-in low-magnification visible-light microscope to assist with pattern and fiducial navigation. The microscope has a field of view of approximately 1.4 mm, horizontally. The two microscope images shown in Fig. 2 were recorded of the same pattern, illuminated separately with (a) bright-field, through-the-lens illumination, and (b) with darkfield illumination from in-vacuum light-emitting diodes (LEDs) positioned 90° apart, to illuminatie the mask from the *x* and *y* directions.

Among the EUV zoneplates installed in SHARP are *navigation* zoneplates, with 225 and 300 magnification. The 300-magnification zoneplate provides a 90-μm-wide field of view, as shown in Fig. 3.

4. ZONEPLATE AND ILLUMINATION SELECTION IN SHARP

Following 8½ months of operation, we can survey the zoneplate and illumination settings requested by SHARP's users. It should not be surprising that these settings match those of the ASML Alpha Demo Tool (ADT),[7] with its 0.25-NA, and the more recent NXE3100 and 3300 tools,[8] which feature 0.33 NA, since those tools are used by several companies in EUV lithography research. Considering 71,000 high-quality images recorded between June 1, 2013 and February 21, 2014, Table 1 describes the relative popularity of each available lens, based on their frequency of use.

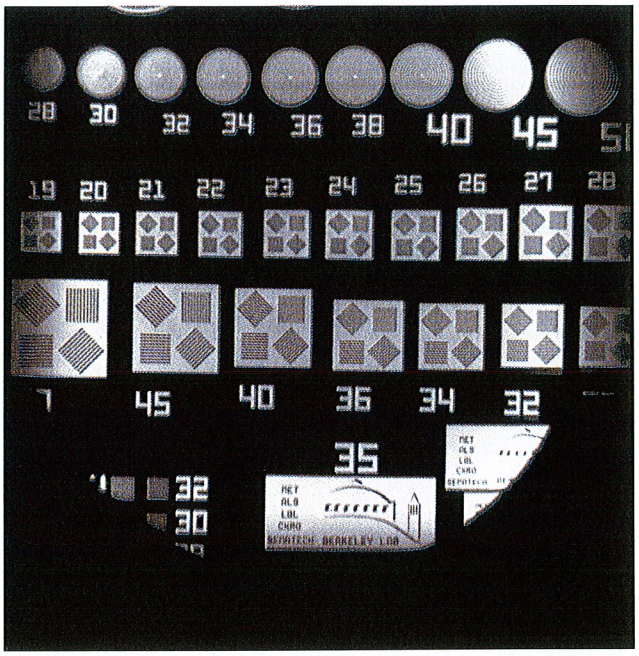

Figure 3. EUV image from a 300×, zoneplate lens used for navigation. The zoneplate has a 1500-μm focal length. Expanding the illuminated area of the mask to match the larger field of view requires that the M_C mirror be scanned through a larger range. The circular shadow of the M_C mirror is visible near the bottom of the image.

Table 1. Relative popularity of the available zoneplate NA values, selected by SHARP users over the first 8½ months of operations. The statistics are based on 71,000 high-resolution images.

4xNA (CRA, degrees)	percentage of total user requests
0.25 (6°)	11.3%
0.33 (6°)	76.2%
0.35 (6°)	7.3%
0.42 (8°)	4.3%
0.50 (8°)	1.0%
0.625 (10°)	0.04%

Figure 4 shows all of the illumination pupil-fill settings requested by users. These include disk fills with various σ (partial coherence) values, *x* and *y* dipole patterns, annular fills, four-leaf *QUASAR*™ patterns with 45° rotation, and so-called *cross-pole* patterns illuminating the *x* and *y* extreme edges of the pupil, respectively. SHARP achieves these pupil fills by scanning the M_A mirror into various patterns during each exposure.[2] Several measured pupil fill patterns are shown in Fig. 5.

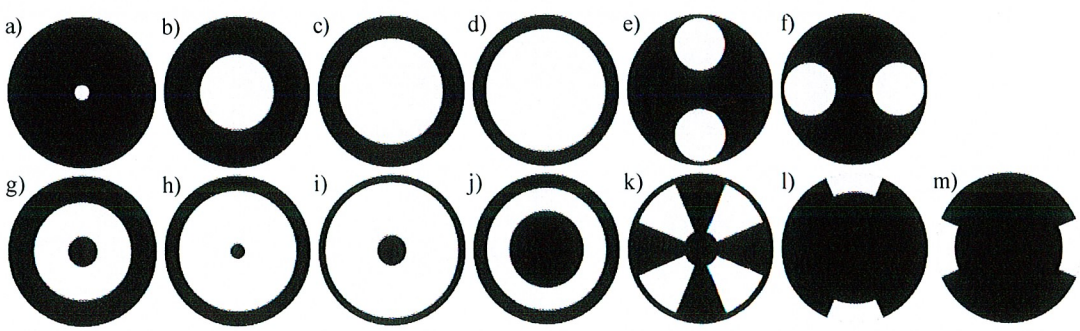

Figure 4. Graphical representation of the most commonly requested (angular) pupil fill patterns in the SHARP illuminator. These fill patterns are referred to as **(a–d)** disk, **(e,f)** dipole, **(g–j)** annular, **(k)** QUASAR™, and **(l,m)** cross pole.

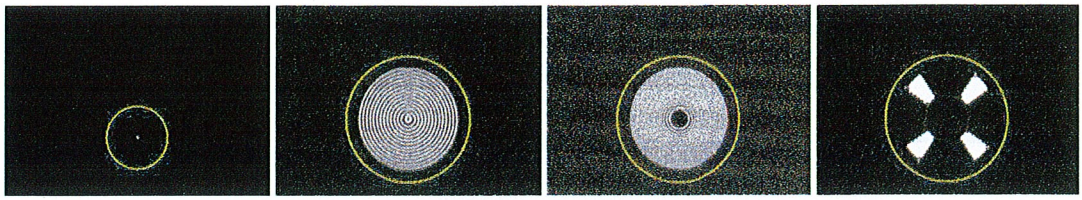

Figure 5. In situ YAG-scintillator microscope images of four illumination pupil-fill patterns, observed in a plane several millimeters below the mask plane. The circle indicates the intended $\sigma = 1$, pupil boundary for each fill pattern. The left image is a coherent fill pattern at a 4xNA of 0.25 with 6° central-ray angle, while the other patterns are recorded for 4xNA of 0.50 with 8° central ray angle.

5. COHERENCE CONTROL

In lithography, illumination coherence, defined by the angular spectrum of the illumination, plays a central role in image formation. SHARP's flexible coherence control system allows demonstrations of this point, and the exploration of subtle changes that occur under different illumination conditions.

Figure 6 contains two through-focus series, recorded of lines with 160-nm CD. As expected, coherent illumination produces so-called 'ringing' and edge artifacts, and a doubling of the lines out of focus. Whereas partially-coherent illumination produces lines with smooth features, and what may be described as a more simple blurring appearance out of focus.

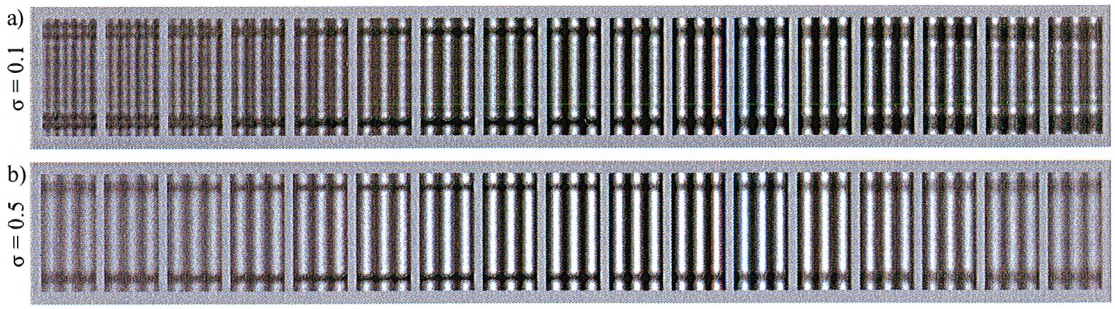

Figure 6. Through-focus image series of 160-nm line segments, recorded with **(a)** high-coherence ($\sigma = 0.1$) and **(b)** partial coherence ($\sigma = 0.5$). The image details are 2-μm tall and the through-focus step size is 0.4 μm, in mask units.

Partial coherence has a strong effect on pattern roughness, including the speckle observed in bright regions of the mask. Figure 7 contains two through-focus series of a 0.5-μm-wide line in a bright region, recorded with coherent and partially coherent light, respectively. Not only is the edge ringing less pronounced in the partially coherent case, but the speckle amplitude is reduced as well.

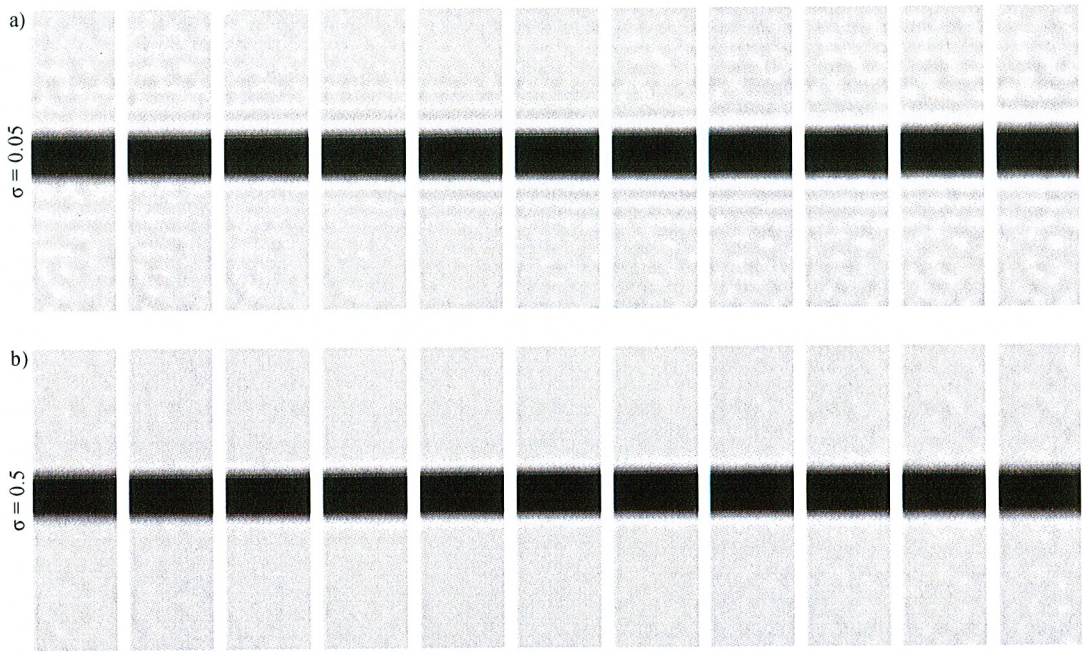

Figure 7. Through-focus image series of a wide, dark line in a bright region, recorded with **(a)** high-coherence ($\sigma = 0.05$) and **(b)** partial coherence ($\sigma = 0.5$). The image details are 3.5-μm tall, the line is 500-nm wide, and the through-focus step size is 0.4 μm, in mask units.

SHARP's ability to switch between coherent and partially coherent illumination nearly instantaneously led us to the observation that coherence control can be used as a focusing aid in the microscope. SHARP is frequently used to image dense line patterns, where finding an unambiguous best focus plane can be challenging. Figure 8 shows examples of a dense line pattern observed through focus with coherent ($\sigma = 0.05$) and then partially coherent ($\sigma = 0.9$) illumination. The measured contrast through-focus, calculated from these image details, is plotted in the graphs to the right. The coherent case shows oscillations in the measured contrast due to the Talbot effect in gratings. The pattern goes through a tone reversal, but returns to high contrast both above and below best focus. However, the partially-coherent case shows a different behavior: the contrast reaches a single peak, in the best focus plane, and the images blur smoothly on both sides of focus.

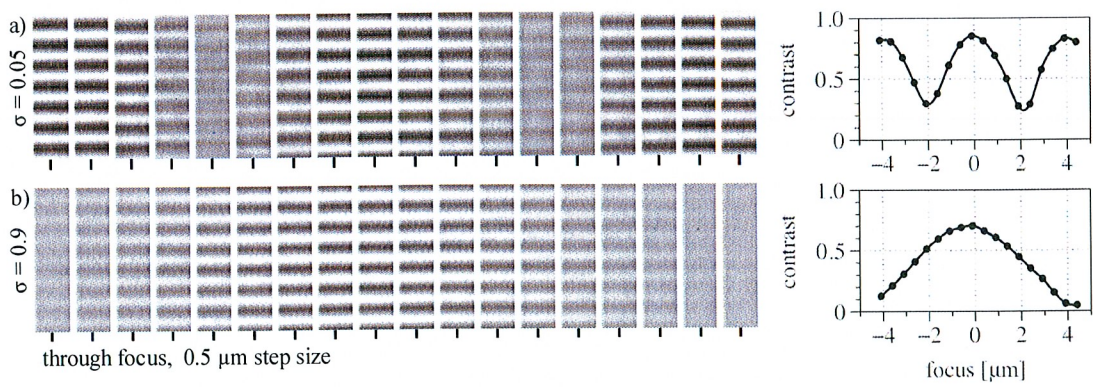

Figure 8. Demonstration of using coherence to identify the best focus plane unambiguously in a dense, repeated pattern. Two through-focus image series of dense lines recorded at the same location, moments apart, with **(a)** high-coherence ($\sigma = 0.05$) and **(b)** partial coherence ($\sigma = 0.9$). Image details are 1.4 μm tall, the lines have 100-nm CD, and the through-focus step size is 0.5 μm, in mask units. Graphs on the right show the measured contrast in each image detail through focus.

6. CREATING ILLUMINATION UNIFORMITY

SHARP creates uniform illumination dynamically, by scanning a focused beam spot through a serpentine pattern during each exposure. SHARP's sweet spot is relatively small (typically 3–5 μm), and creating a uniform (flat) illumination profile across that region is essential for accurate reproducible analysis of the image pattern profiles.

6.1 Uniformity demonstration

Figure 9a is an image of an all-bright region on a mask with the M_A scanning to provide disk-fill with a partial coherence of $\sigma = 0.5$, and the M_C scanner held static. (Filtering has been applied to remove the speckle from the image.) Here, in an image that is 30.7-μm wide we see that the beam subtends 8.4 × 7.1-μm FWHM, with a smooth peak.

Uniformity is achieved by scanning this pattern spatially. Scanning the M_C mirror through small angles (tens of micro-radians) produces a negligible effect on the beam angle, but generates a beam displacement of many micrometers on the mask surface. An example scan pattern is shown in Fig. 9b. Starting near the lower-left corner, the beam first performs an x-direction scan, stepping in the $+y$ direction in eight passes, with discrete y values. The beam then returns to the $-y$ edge with eight more steps, interleaved with the previous y positions, and shifted in y by one-half step. The pattern just described is then rotated by 90° and repeated with continuous y scanning and discrete x steps. The resulting, measured illumination is shown in Fig. 9c.

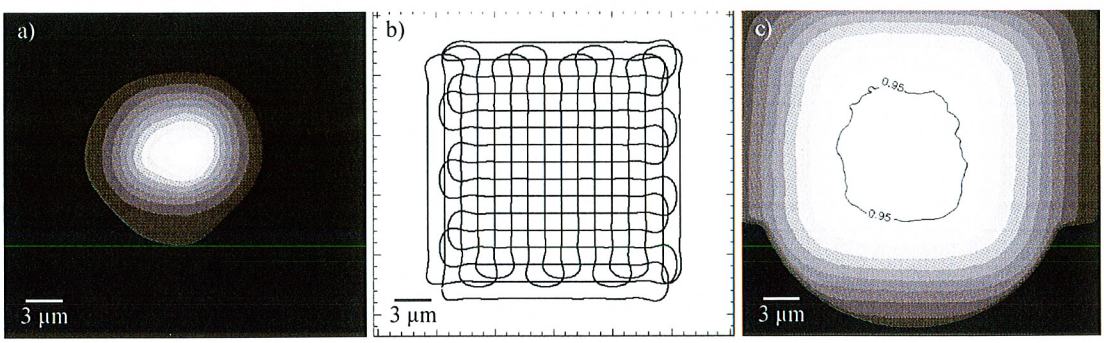

Figure 9. Demonstration of illumination uniformity created by scanning a small, focused beam on a bright region of a mask. Each image is 30.7 μm wide, corresponding to the full width of the CCD at 900 magnification. Gray-level contours represent 10% intensity increments with respect to the peak value. **(a)** The beam as it appears with $\sigma = 0.5$ disk fill, and a static M_C mirror (i.e. no scanning). The full-width at half-maximum size is 8.4 × 7.1-μm. **(b)** An interleaved xy raster pattern with 16 scan rows and columns. **(c)** Measured, uniformly illuminated central region. The thin black line shows the intensity contour at 95% of the peak level.

This programmed, scanning illumination strategy provides additional flexibility for SHARP. The size of the illuminated region can be changed and expanded at will; up to 100-μm width has been demonstrated (with an associated loss of flux density). Plus the speed of the scanning beam can be modulated at different spatial positions to produce illumination gradients in arbitrary directions and with linear or higher-ordered shapes, should that ever prove necessary.

6.2 Power and uniformity analysis

To assess power stability and illumination uniformity in SHARP, a series of 11 images was recorded through focus at a bright region of the mask, matching the normal mode of data collection. Illumination uniformity was generated using the scan pattern and coherence settings described above. From each image, we extract and study centered square regions with 3-, 4-, and 5-μm widths, respectively. The results or power and uniformity analysis are plotted in Fig. 10.

The average power is calculated by integrating the total signal within the extracted square regions of each image, and normalizing to the overall average value at each size. The total power values are proportional to the average pixel-by-pixel intensity. In this series, the variance in the measured power in the 3, 4, and 5 μm regions is 0.97%, 0.84%, and 0.75%, respectively. In other words, a 1% RMS power fluctuation can be expected with this pattern and illumination settings.

We define *uniformity* as the maximum absolute intensity deviation from the average value (whether greater or less than the average) with the average value normalized to unity. To eliminate spurious contributions from speckle, a 2nd order

polynomial fit to the intensity values in the square regions is used in the analysis. In this series, the average uniformity in the measured 3, 4, and 5 μm regions is 98.40%, 98.31%, and 97.90%, respectively. This implies spatial intensity variations within the extracted regions, on average, of ±1.60%, ±1.69%, and ±2.1%, respectively.

Further development of optimal scan patterns and sources of the variability may allow us to improve the power stability and illumination uniformity levels.

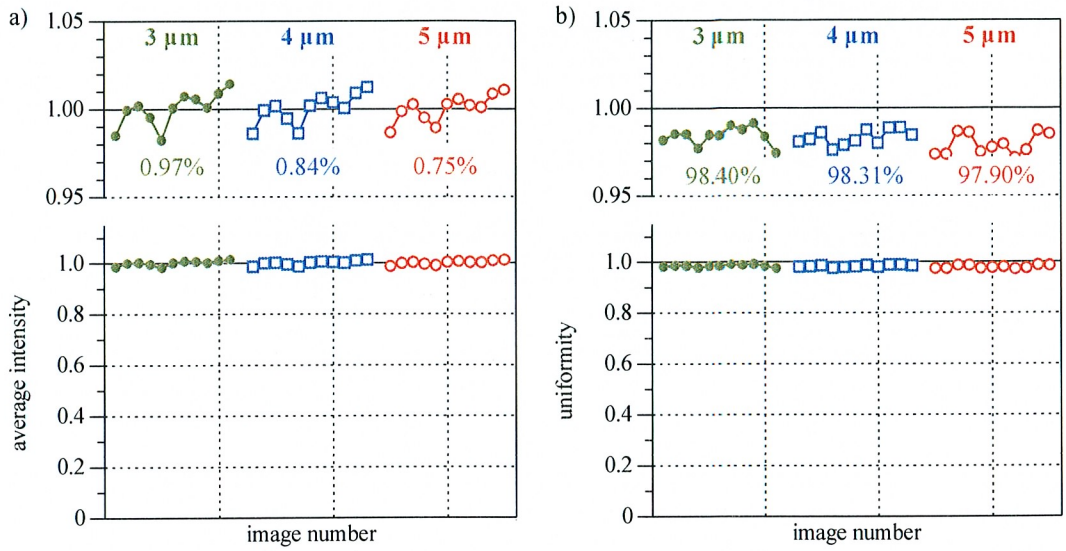

Figure 10. Results of an 11-image, through-focus series study on **(a)** illumination power stability, and **(b)** illumination uniformity, within centered square regions measuring 3-, 4-, and 5-μm wide. In **(a)**, the percentage values represent the variance in the integrated power with respect to the normalized, average value in the series. In **(b)**, the percentage values are the average uniformity within each series. The plots on top are magnified versions of the data below.

7. DATA COLLECTION RATE

During normal operations SHARP routinely collects through-focus series at a rate of approximately 8 to 10 series per hour. While minor gains in speed (5–10%) may be possible, we believe that SHARP is running close to its maximum throughput, with the current through-focus series specifications.

When masks are first loaded into SHARP, we perform a series of steps to establish the coordinate system for measurement. In most cases, this involves finding three or more widely spaced, known fiducial marks. Once established, this *xyz* coordinate system is used for full-mask navigation, including coarse focusing.

Following this alignment, in routine operation, the data-collection rate depends on two parts: (a) navigation and fine alignment, and (b) series collection. Navigation is guided by a pre-loaded experiment plan and software that can jump to any position on the mask to within a few microns. Fine alignment is performed manually, by eye, and involves centering the target location on the zoneplate's sweet spot location. Focus is tested to ensure that the series will be centered in *z*. If it has drifted, the illumination is adjusted, to center it on the sweet spot. The pupil-fill for each measurement is also contained in the experiment plan and can be set with a button click.

Series data collection is automated. Users typically request through-focus series with 17 to 25 images, with longitudinal step sizes of 0.4 or 0.5 μm, in mask units. For high-quality imaging, SHARP's exposure time varies from 5 to 8 seconds, depending on the mask pattern and illumination properties. Between each exposure, there is CCD-readout time, zoneplate *z*-stage motion, and settling time to accommodate before the next image is recorded.

Figure 9 is a chronological plot of 28 through-focus series collected during the span of one afternoon. We recorded 476 images, with 17 images per series. Between each series there is a gap for navigation and fine alignment. In this instance, the overall data collection rate was 8.91 series per hour.

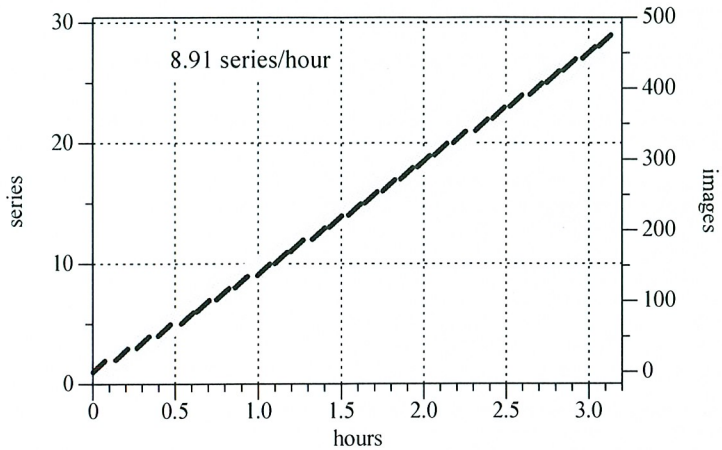

Figure 11. An example of the data collection rate from three hours of measurement. We recorded 28 series with 17 images per series, totaling 476 images. The start time of each 5- second exposure is plotted. Between each 17-image series, the operator manually navigates to the next measurement positions and performs fine alignment, leading to the gaps in the plot. The average rate in this instance is 8.91 series per hour.

Data collection rate statistics for two masks measured in January 2014 are shown in Table 2. One was a blank mask with defect locations marked by 5-µm punch-marks close to the defects. The other mask is a patterned mask with an array of measurement locations and labels within 20 µm of the measurement points.

Table 2. Measured time in minutes between the end of one series and the start of the next, for two different kinds of masks. This data was collected from two days in January 2014.

	blank mask with marked defects	patterned mask with programmed defect array
number of series measured	48	57
median [min]	2.36	1.81
average [min]	2.67	2.63
min [min]	1.17	1.34
max [min]	10.44	16.32

In both cases studied here, the median navigation and fine-alignment times were close to 2 minutes, with minimum values just above 1 minute. Occasional longer times in the dataset are due to a variety of causes: navigation uncertainty, planning discussions with team members, phone calls with remote users, resolving a software problem, or the need to step away from the experiment for a few minutes when another operator is not available to cover.

Some improvements in data-collection rate could come through navigation and alignment efficiency, or from an optimized fiducialization procedure performed when masks are loaded. We also recommend that the number and spacing of through-focus series steps be re-considered. In some cases, it may be possible to reduce the number of steps and/or increase the step size and to acquire adequate data for a given application or analysis.

8. CONCLUSION

In its first 8½ months of user operations, SHARP has become an active contributor to EUV mask research programs within the SEMATECH member companies, conducting research in nearly all areas of mask development. Its flexible illumination and imaging conditions enable it to emulate current and future lithography tools. Since illumination coherence strongly influences imaged pattern roughness, defect printability, and pattern edge shapes, SHARP can be used in the development and validation of defect repair solutions and pattern enhancement strategies. Improvements in SHARP's illumination uniformity and stability have improved the measurement of line and pattern features; further gains may be possible by engineering different scan paths. Observations of the behavior of through-focus image formation under different partial coherence levels gave rise to improved focusing techniques that have improved measurement efficiency. We believe that SHARP's overall data rate of between 8 and 10 series per hour is close to its

maximum rate under current experimental conditions. Some improvement may be possible by optimizing the series data collection (specifically the number of images, and the focal step size) for different pattern types and illumination conditions.

SHARP is well positioned to contribute to the ongoing strategy discussion on EUV pattern scaling at future technology nodes: whether to increase the mask-side NA and maintain the 4× projection-optics' magnification, or to increase the magnification ratio and move to larger mask sizes.

9. ACKNOWLEDGEMENT

This work is funded by SEMATECH, and performed by University of California Lawrence Berkeley National Laboratory under the auspices of the U.S. Department of Energy, Contract No. DE-AC02-05CH11231. The authors gratefully acknowledge the support of SEMATECH project leaders and managers, David Chan, Andy Ma, Chihcheng Lin, Bryan Rice, Frank Goodwin, Stefan Wurm, and Kevin Cummings. QUASAR™ is a trademark of ASML, Netherlands.

REFERENCES

[1] K. A. Goldberg, I. Mochi, M. Benk, A. P. Allezy, *et al.*, "Commissioning an EUV mask microscope for lithography generations reaching 8 nm," *Proc. SPIE* **8679**, 867919, (2013).

[2] K. A. Goldberg, I. Mochi, M. P. Benk, C.C. Lin, *et al.*, "The SEMATECH high-NA actinic reticle review project (SHARP) EUV mask-imaging microscope," *Proc. SPIE* **8880**, 88800T, (2013).

[3] K. A. Goldberg, I. Mochi, S. B. Rekawa, N. S. Smith, J. B. Macdougall, P. P. Naulleau, "An EUV Fresnel zoneplate mask-imaging microscope for lithography generations reaching 8 nm," *Proc. SPIE* **7969**, 79691O (2011).

[4] K. A. Goldberg, I. Mochi, M. P. Benk, A. P. Allezy, *et al.*, "Creating an EUV Mask Microscope for Lithography Generations Reaching 8 nm," *Precision Engineering and Mechatronics Supporting the Semiconductor Industry*, 4–7 (2012).

[5] K. A. Goldberg, I. Mochi, M. Benk, A. P. Allezy, *et al.*, "Commissioning an EUV mask microscope for lithography generations reaching 8 nm," *Proc. SPIE* **8679,** 867919 (2013).

[6] K. A. Goldberg, I. Mochi, "Wavelength-Specific Reflections: A Decade of EUV Actinic Mask Inspection Research," *J. Vac. Sci. Technol. B* **28** (6), C6E1-10 (2010).

[7] H. Meiling, H. Meijer, V. Banine, R. Moors, *et al.*, "First performance results of the ASML alpha demo tool," *Proc. SPIE* **6151**, 615108 (2006).

[8] R. Peeters, S. Lok, E. van Alphen, N. Harned, *et al.*, "ASML's NXE platform performance and volume introduction," *Proc. SPIE* **8679**, 86791F (2013).

DISCLAIMER

This document was prepared as an account of work sponsored by the United States Government. While this document is believed to contain correct information, neither the United States Government nor any agency thereof, nor The Regents of the University of California, nor any of their employees, makes any warranty, express or implied, or assumes any legal responsibility for the accuracy, completeness, or usefulness of any information, apparatus, product, or process disclosed, or represents that its use would not infringe privately owned rights. Reference herein to any specific commercial product, process, or service by its trade name, trademark, manufacturer, or otherwise, does not necessarily constitute or imply its endorsement, recommendation, or favoring by the United States Government or any agency thereof, or The Regents of the University of California. The views and opinions of authors expressed herein do not necessarily state or reflect those of the United States Government or any agency thereof or The Regents of the University of California.